INTERNATIONAL JOURNAL OF
NUMERICAL ANALYSIS AND MODELING
Volume 15, Number 1-2, Pages 213–227

UNIFORM L^p-BOUND OF THE ALLEN–CAHN EQUATION AND ITS NUMERICAL DISCRETIZATION

JIANG YANG, QIANG DU, AND WEI ZHANG*

Abstract. We study uniform bounds associated with the Allen–Cahn equation and its numerical discretization schemes. These uniform bounds are different from, and weaker than, the conventional energy dissipation and the maximum principle, but they can be helpful in the analysis of numerical methods. In particular, we show that finite difference spatial discretization, like the original continuum model, shares the uniform L^p-bound for all even p, which also leads to the maximum principle. In comparison, a couple of other spatial discretization schemes, namely the Fourier spectral Galerkin method and spectral collocation method preserve the L^p-bound only for $p = 2$. Moreover, fully discretized schemes based on the Fourier collocation method for spatial discretization and Strang splitting method for time discretization also preserve the uniform L^2-bound unconditionally.

Key words. Allen–Cahn Equations, maximum principle, operator splitting, uniform L^p-bound, Fourier spectral methods.

1. Introduction

We consider the standard Allen–Cahn (AC) equation in this paper, which is given as follows

$$\begin{aligned} &\frac{\partial u}{\partial t} = \epsilon^2 \Delta u - f(u), \quad && \mathbf{x} \in \Omega, t \in (0, T], \\ &u(\mathbf{x}, 0) = u_0(\mathbf{x}), && \mathbf{x} \in \bar{\Omega}, \end{aligned} \tag{1}$$

where $u = u(x, t)$ is a real-valued scalar function, the nonlinear term is given by $f(u) = u^3 - u$, the parameter $\epsilon > 0$ characterizes the width of diffuse interface, and Ω is a bounded domain in R^d. We restrict our attention to the periodic boundary condition with Ω being the unit cell. The Allen–Cahn equation can be viewed as an L^2-gradient flow of the following Ginzburg-Landau free energy functional

$$E(u) = \int_\Omega \left(\frac{1}{2} \epsilon^2 |\nabla u|^2 + F(u) \right) dx, \tag{2}$$

where $F(u)$ is taken as the typical double well potential $F(u) = \frac{1}{4}(u^2 - 1)^2$ so that $f(u) = F'(u)$. We also assume that the initial data $u_0 = u_0(x)$ takes value between the energy wells, i.e., bounded by the constant 1.

The Allen–Cahn equation has been introduced by Allen and Cahn in [1] to describe the motion of anti-phase boundaries in crystalline solids. The equation also bears other names, for example, the Ginzburg-Landau equation where the unknown solution may be real, complex, or vector-valued [8, 21]. It is now a basic model equation for the diffuse interface (phase field) approach developed to study phase transitions and interfacial dynamics in materials science as well as various problems in many other applications [4, 7]. There have also been extensive numerical studies of phase field and diffuse interface models, see, e.g. [6, 16, 20].

Received by the editors January 20, 2017 and, in revised form, March 13, 2017.
2000 *Mathematics Subject Classification.* 65M70, 65R20.
*Corresponding author.

One of the important issues concerning numerical solution of differential equations is the stability of numerical schemes. For nonlinear models, a priori bounds on the discrete solutions are often important to the numerical stability. Given AC being a typical gradient flow, we have

$$\frac{d}{dt}E = -\|u_t\|_2^2 \leq 0 \quad \text{and} \quad E(t) \leq E(0),$$

which represents the energy bound of the original continuum model. The preservation of such nonlinear energy bounds by numerical approximations often dominates the discussions in numerical analysis, In [11], Eyre proposed an unconditionally stable energy convex splitting scheme for general gradient flows, but it is only first order. Some recent stability analysis can be found in[12, 13, 14, 24, 28, 29], where most authors again focused on the energy dissipation.

Another intrinsic bound for the Allen–Cahn equation is the point-wise bound in the form of a maximum principle, see, e.g., [10]. Specifically, if the initial data $u_0(x)$ takes value between the energy wells, i.e., bounded by the constant 1, then the time-dependent solution of the Allen–Cahn equation is also bounded by constant 1. Such a property can be preserved numerically on the discrete level, see for example [5, 27] for discussions on fully discrete finite volume and finite difference approximations. The discrete maximum principle was further extended to generalized Allen–Cahn equations and fractional Allen–Cahn equations [18, 23]. In these works, the space Laplace operator is discretized by central finite difference. Similar results have been established for finite volume schemes as well as finite element methods with mass lumping based on Voronoi-Delaunay meshes, see [6] and the references cited therein. However, it is known that the maximum principle can not be preserved in general by spectral methods, since the spectral projection itself may fail to retain point-wise bounds. Hence, we do not expect that spectral methods preserve the maximum principle for nonlinear Allen–Cahn equations.

In this paper, we present some bounds on solutions other than the energy bound and maximum principle for the Allen–Cahn equation and its numerical discretization. Specifically, we consider weaker L^p-bounds. First, we define the L^p-average norm $\|\!|\cdot|\!\|_p$ of u in the fixed domain Ω for any $p > 0$,

$$\|\!|u|\!\|_p = \frac{1}{S_\Omega}\|u\|_{L^p(\Omega)}^p = \frac{1}{S_\Omega}\int_\Omega |u|^p dx, \tag{3}$$

where S_Ω is the volume of the domain Ω. Given the assumed bounds on the initial data, by applying the maximum principle directly, we can obtain

$$\|\!|u|\!\|_p(t) = \frac{1}{S_\Omega}\int_\Omega |u(x,t)|^p dx \leq \frac{1}{S_\Omega}\int_\Omega 1 dx = 1, \tag{4}$$

which is uniform not only in space and time, but also with respect to the domain Ω, the diffuse interface width ϵ and the exponent p. This uniform L^p-bound is, of course, weaker than the maximum principle. On the other hand, the uniform L^p-bound implies the maximum principle if it holds for a sequence of p that goes to infinity. The larger p one can pick, the closer L^p-bound is to the maximum principle.

Computationally, we are often interested in constructing discrete numerical schemes that preserve the properties of the continuum equations as much as possible. However, this is not always possible for complex systems. Hence, it is interesting to know to what extent, weaker results can be established which may still allow the numerical schemes to provide reliable computational predictions. For example, it is obvious that there could be more flexibility designing numerical schemes to preserve

the uniform L^p-bound instead of the maximum principle. In this paper, we show that the semi-discretized system with finite difference for spatial discretization can preserve the uniform L^p-bound for all even integer p, thus leading to the discrete maximum principle as p goes to infinity. On the other hand, the semi-discrete system with Fourier Galerkin/collocation methods for spatial discretization only preserves the uniform L^2-bound and fails to preserve the maximum principle.

The rest of the paper is organized as follows. In Section 2, we first prove the uniform L^p-bound for the continuum Allen–Cahn equations without using maximum principle. The performances of semi-discrete schemes on preserving the uniform L^p-bound are studied in Section 3, including finite difference methods and Fourier Galerkin/collocation methods. In the following section, we first review some regular time stepping schemes, and then adopt operator splitting for the time discretization. We show that the second order Strang splitting can preserve the uniform L^2-bound unconditionally. Some numerical examples are carried out to verify the numerical analysis in Section 5, and some concluding remarks are given in the final section, in particular, with respect to the extension to vector valued Allen–Cahn or Ginzburg-Landau systems.

2. Uniform L^p-bound for continuum equations

In this section, we will establish the L^p-bound for continuum Allen–Cahn equations for even p. We start with a useful lemma.

Lemma 1. *For a nonnegative function $y(t)$, $y(t) \in C^1[0, +\infty)$ satisfies*

$$\begin{cases} \frac{dy}{dt} \le c(y - y^2), \\ y(0) = y_0, \end{cases}$$

where c is a positive constant and $0 \le y_0 < 1$. Then

$$y(t) \le 1, \quad \forall t \ge 0.$$

Proof. Since $0 \le y(0) < 1$ and $y = y(t)$ is continuous, there exists a $\alpha > 0$ such that $y(t) \le 1$, for any $t \in [0, \alpha)$. If the conclusion of the lemma does not hold, then there exists a $t_1 > \alpha$ such that $y(t_1) > 1$. Let us define

$$\beta = \min\{\ t \mid y(t) = 1 \quad \text{and} \quad \exists \delta(t) > 0 \quad \text{s.t.} \quad y(s) > 1, \quad \forall s \in (t, t + \delta(t))\},$$

then it is easy to see $\alpha \le \beta < t_1$ and $y(\beta) = 1$. Moreover, for $t \in (\beta, \beta + \delta(\beta)]$, we have $y(t) > 1$. Thus,

$$y'(t) \le c(y - y^2) < 0, \quad t \in (\beta, \beta + \delta(\beta)].$$

Consequently,

$$\begin{aligned} y(\beta + \tfrac{1}{2}\delta(\beta)) &= \textstyle\int_\beta^{\beta+\delta(\beta)/2} y'(s)ds + y(\beta) \\ &\le \textstyle\int_\beta^{\beta+\delta(\beta)/2} c(y(s) - y^2(s))ds + 1 \le 1. \end{aligned}$$

However, we know that $y(\beta + \frac{1}{2}\delta(\beta)) > 1$, which leads to a contradiction. This establishes the lemma. □

We next prove that solutions to the continuous model (1) satisfy the uniform L^p-bound without using the maximum principle.

Theorem 1. *For the Allen–Cahn equation (1), if the initial data $u_0 = u_0(x)$ satisfies*

$$\max_{\boldsymbol{x} \in \bar{\Omega}} |u_0(\boldsymbol{x})| \le 1, \tag{5}$$

then the solution $u = u(t,x)$ satisfies the L^p-bound for any even integer p, that is,

$$\|\!|u(t,\cdot)|\!\|_p \le 1, \quad \forall t \ge 0. \tag{6}$$

Proof. First we prove that (6) holds when $p = 2$. Using the periodic boundary condition and taking L^2 inner product of the Allen–Cahn equation (1) with u yields

$$\frac{1}{2}\frac{d\|u\|_2^2}{dt} = -\epsilon^2\|\nabla u\|_2^2 + \|u\|_2^2 - \|u^2\|_2^2, \tag{7}$$

where we have taken the fact that $(u, u^3) = \|u^2\|_2^2$. By letting $\phi = 1$ and $\psi = u^2$ and using the Cauchy-Schwarz inequality, we arrive at

$$\|u^2\|_2^2 = \frac{1}{S_\Omega}\|\phi\|_2^2\|\psi\|_2^2 \ge \frac{1}{S_\Omega}|(\phi,\psi)|^2 = \frac{1}{S_\Omega}\|u\|_2^4. \tag{8}$$

Dividing (7) by S_Ω and combining with (8), we get

$$\frac{d\|\!|u|\!\|_2}{dt} \le 2(\|\!|u|\!\|_2 - \|\!|u|\!\|_2^2). \tag{9}$$

Since the initial data $u_0(x) \in C(\Omega)$ satisfies (5), we have $0 \le \|\!|u(0,\cdot)|\!\|_2 \le 1$. If $\|\!|u(0,\cdot)|\!\|_2 = 1$, then $u(t,x) \equiv u_0(x) \equiv \pm 1$ for all t. Thus $\|\!|u(t,\cdot)|\!\|_2 \equiv 1$. For the case $0 \le \|\!|u(0,\cdot)|\!\|_2 < 1$, we have

$$\|\!|u(t,\cdot)|\!\|_2 \le 1, \quad \forall t \ge 0 \tag{10}$$

thanks to Lemma 1. We are ready to complete the proof by mathematical induction for $p > 2$. We assume (6) holds for $p = 2k-2$ as $k > 1$, i.e.

$$\|\!|u|\!\|_{2k-2} = \frac{1}{S_\Omega}\|u^{k-1}\|_2^2 \le 1. \tag{11}$$

To prove that it still holds for $p = 2k$, we take the L^2 inner product of the Allen–Cahn equation (1) with u^{2k-1} to get

$$\frac{1}{2k}\frac{d\|u\|_{2k}^{2k}}{dt} = -\epsilon^2(2k-1)\|u^{k-1}\nabla u\|_2^2 + \|u\|_{2k}^{2k} - (u^3, u^{2k-1}). \tag{12}$$

With (11), the last term on the right-hand side of the above equation can be estimated as

$$\begin{aligned}(u^3, u^{2k-1}) &= \|u^{k+1}\|_2^2 \ge \left(\frac{1}{S_\Omega}\|u^{k-1}\|_2^2\right)\|u^{k+1}\|_2^2 \\ &\ge \frac{1}{S_\Omega}(u^{k-1}, u^{k+1})^2 = \frac{1}{S_\Omega}\left(\|u\|_{2k}^{2k}\right)^2.\end{aligned}$$

Hence, we arrive at

$$\frac{1}{2k}\frac{d\|u\|_{2k}^{2k}}{dt} \le \|u\|_{2k}^{2k} - \frac{1}{S_\Omega}\left(\|u\|_{2k}^{2k}\right)^2. \tag{13}$$

Dividing (13) by S_Ω gives a similar inequality as (9),

$$\frac{d\|\!|u|\!\|_{2k}}{dt} \le 2k(\|\!|u|\!\|_{2k} - \|\!|u|\!\|_{2k}^2).$$

Meanwhile, since $\|\!|u(0)|\!\|_{2k} \le 1$, the remaining derivation can be done in the same way as in the case when $p = 2$. □

The L^p-bound is weaker than the maximum principle. However, this uniform L^p-bound offers us one way to prove the maximum principle as p goes to infinity.

Corollary 1. (Maximum principle) *For the Allen–Cahn equation (1), if the initial data $u_0 = u_0(x)$ satisfies (5), then the solution $u = u(t,x)$ satisfies the maximum principle, that is,*

$$\|u(t,\cdot)\|_\infty \le 1, \quad \forall t \ge 0. \tag{14}$$

It is noted that although we have exclusively focused on the periodic boundary condition case, from the derivations presented in this section one can see that the results given here remain valid for homogeneous Neumann/Dirichlet boundary conditions as well.

3. Semi-discrete schemes and uniform L^p-bound

In this section, we investigate the uniform L^p-bound of semi-discrete schemes, including central finite difference, Fourier Galerkin method, and Fourier collocation method for the spatial discretization. To demonstrate the main idea, without loss of generality, we only consider problems defined on $[0, 2\pi]$ to avoid the use of more complicated tensor notation and multiple indices. Besides more involved notations, our analysis can be extended to both 2D and 3D cases trivially.

3.1. Finite difference methods and L^p-bound. We first use the central finite difference method to discretize the Laplace operator. We take the uniform mesh on $[0, 2\pi]$, i.e. $x_j = \frac{2\pi j}{N}, j = 0, 1, \cdots, N-1$. Thus, the discrete operator D_h can be viewed as the composition of one forward difference D^+ and one backward difference D^-, i.e., $D_h = D^+D^-$. In matrix form, if we denote D^- by D_1, then D^+ can be represented by $-D_1^T$, hence $D_h = -D_1^T D_1$ with the matrices given as follows for the periodic boundary condition:

$$D_h = \frac{1}{h^2}\begin{bmatrix} -2 & 1 & & & 1 \\ 1 & -2 & 1 & & \\ & \ddots & \ddots & \ddots & \\ & & 1 & -2 & 1 \\ 1 & & & 1 & -2 \end{bmatrix}_{N\times N},$$

$$D_1 = \frac{1}{h}\begin{bmatrix} 1 & & & & -1 \\ -1 & 1 & & & \\ & \ddots & \ddots & \ddots & \\ & & -1 & 1 & \\ & & & -1 & 1 \end{bmatrix}_{N\times N}.$$

Let $U_j(t)$ denote the approximation of $u(t, x_j)$, $U = (U_0, U_1, \cdots, U_{N-1})^T$, and $U^{\cdot k} = (U_0^k, U_1^k, \cdots, U_{N-1}^k)^T$. Then we end up with the following nonlinear ordinary differential equation (ODE) system

$$\begin{cases} \frac{dU}{dt} = \epsilon^2 D_h U + U - U^{\cdot 3}, \\ U(0) = U^0 = (u_0(x_0), u_0(x_1), \cdots, u_0(x_{N-1}))^T, \end{cases} \tag{15}$$

Lemma 2. *For the discrete $N \times N$ matrix D_h defined above, we have*

$$\left(U^{\cdot(2p-1)}\right)^T D_h U \le 0, \quad \forall\, U \in R^N, \quad p \ge 1. \tag{16}$$

Proof. Since $D_h = -D_1^T D_1$, we get

$$\left(U^{\cdot(2p-1)}\right)^T D_h U = -(D_1 U^{\cdot(2p-1)})^T D_1 U.$$

The jth element of $D_1U^{\cdot(2p-1)}$ and D_1U are given respectively as follows

$$\left(D_1U^{\cdot(2p-1)}\right)_j = \frac{U_j^{(2p-1)} - U_{j-1}^{(2p-1)}}{h}, \quad (D_1U)_j = \frac{U_j - U_{j-1}}{h}.$$

Consequently,

$$\left(D_1U^{\cdot(2p-1)}\right)_j (D_1U)_j \geq 0.$$

Thus, a summation over j leads to (16). □

On the discrete level, we can define the corresponding average L^p-norm as

$$|||U|||_p = \frac{1}{2\pi} h \sum_{j=0}^{N} |U_j|^p = \frac{1}{N} \sum_{j=0}^{N} |U_j|^p.$$

Theorem 2. *For the Allen–Cahn equation (1), if the initial data $u_0 = u_0(x)$ satisfies* (5)*, then the numerical solution $U(t)$ given by the semi-discrete finite difference method (15) satisfies the uniform L^p-bound for any even number p in the sense that*

$$|||U(t)|||_p \leq 1, \quad \forall t \geq 0. \tag{17}$$

Furthermore, we have

$$\|U(t)\|_\infty \leq 1, \quad \forall t \geq 0. \tag{18}$$

The proof for (17) is similar to the continuum case, thanks to Lemma 2. We skip the details here. For (18), i.e., discrete maximum principle, we can derive it from (17) .

3.2. Fourier Galerkin method and the uniform L^2-bound. We now consider the semi-discrete Fourier Galerkin approximation of the Allen–Cahn equation with the periodic boundary condition on the domain $[0, 2\pi]$. That is, we seek real solutions $u_N(t, x)$ in the space $\hat{B}_N = \text{span}\{e^{inx}\}_{|n|\leq N}$, i.e.,

$$u_N(t, x) = \sum_{|n|\leq N} a_n(t) e^{inx}, \tag{19}$$

where the coefficients $a_n(t)$ are solved by making the residual

$$R_N(t, x) = \frac{\partial u_N(t, x)}{\partial t} - \left(\epsilon^2 \frac{\partial^2 u_N(t, x)}{\partial x^2} + u_N(t, x) - (u_N(t, x))^3\right), \tag{20}$$

orthogonal to $\hat{B}_N$. We define the L^2-Fourier projection $P_N[\omega](x)$ of $\omega \in L^1[0, 2\pi]$ given by

$$P_N[\omega](x) = \sum_{|n|\leq N} \hat{\omega}(n) e^{inx}, \quad \hat{\omega}(n) := \frac{1}{2\pi} \int_0^{2\pi} \omega(x) e^{-inx} dx.$$

The orthogonality is then equivalent to $P_N R_N(t, x) = 0$, i.e.,

$$\frac{\partial u_N(t, x)}{\partial t} = \epsilon^2 \frac{\partial^2 u_N(t, x)}{\partial x^2} + u_N(t, x) - P_N[u_N^3(t, x)], \tag{21}$$

where we have taken into account that all terms in the residual (20) are in $\hat{B}_N$ except for $u_N^3(t, x)$. According to (3), the L^2-average norm $|||u_N(t, \cdot)|||_2$ of $u_N(t, x)$ is given as

$$|||u_N(t, \cdot)|||_2 = \frac{1}{2\pi} \|u_N(t, \cdot)\|_2^2 = \frac{1}{2\pi} \int_0^{2\pi} |u_N(t, x)|^2 dx = \sum_{|n|\leq N} |a_n(t)|^2. \tag{22}$$

For the projection operator P_N we have the following lemma.

Lemma 3. *For the real-valued solution $u_N(t,x)$ given in the form of (19), we have*

$$\left(P_N[u_N^3(t,\cdot)], u_N(t,\cdot)\right) \geq 2\pi |||u_N(t,\cdot)|||_2^2. \tag{23}$$

Proof. It is easy to check that

$$\left(P_N[u_N^3(t,\cdot)], u_N(t,\cdot)\right) = \left(u_N^3(t,\cdot), u_N(t,\cdot)\right).$$

Since $u_N(t,x)$ is real-valued, we have the fact that

$$\begin{aligned}\left(u_N^3(t,\cdot), u_N(t,\cdot)\right) &= \|u_N^2(t,\cdot)\|_2^2 = \tfrac{1}{2\pi}\|1\|_2^2 \, \|u_N^2(t,\cdot)\|_2^2 \\ &\geq \tfrac{1}{2\pi}|(u_N^2(t,\cdot),1)|^2 = \tfrac{1}{2\pi}\|u_N(t,\cdot)\|_2^4 = 2\pi |||u_N(t,\cdot)|||_2^2.\end{aligned}$$

Thus, we get (23). □

Theorem 3. *For the Allen–Cahn equation (1), if the initial data $u_0 = u_0(x)$ satisfies*

$$|||u_0|||_2 \leq 1,$$

then the solution $u_N(t,x)$ given by the Fourier-Galerkin method (21) satisfies the uniform L^2-bound in the sense that

$$|||u_N(t,\cdot)|||_2 \leq 1, \quad \forall t \geq 0. \tag{24}$$

Proof. Taking the L^2 inner product of equation (21) with $u_N(t,x)$ yields

$$\frac{1}{2}\frac{d\|u_N\|_2^2}{dt} = -\epsilon^2 \|\frac{\partial u_N}{\partial x}\|_2^2 + \|u_N\|_2^2 - (P_N[u_N^3], u_N).$$

By Lemma 3, we have the similar inequality as (9)

$$\frac{d|||u_N|||_2}{dt} \leq 2(|||u_N|||_2 - |||u_N|||_2^2).$$

We can then get (24) by using the same argument presented in the proof of the Theorem 1 . □

We do not expect the uniform L^p-bound for the Fourier Galerkin methods for p greater than 2. This is because, for all even number $p > 2$, we generally have

$$(P_N[u_N^3], u_N^{p-1}) \neq (u_N^3, u_N^{p-1}), \tag{25}$$

However, for any real-valued triangular polynomial u_N the following inequality still holds

$$\left(\frac{\partial^2}{\partial x^2} u_N, u_N^{2p-1}\right) \leq 0, \quad p \geq 1. \tag{26}$$

Hence, Fourier Galerkin methods generally fail to preserve the maximum principle for the Allen–Cahn equation due to (25).

On the other hand, we note that in the absence of nonlinearity, then the Fourier Galerkin methods may still be able to preserve suitable estimates for linear models. The latter is not directly related to the study of Allen-Cahn models but could be of its own independent interest. For example, the next corollary immediately follows from (26).

Corollary 2. (Uniform bound for the linear heat equation) *If the heat equation $u_t = \epsilon\Delta u$ with a periodic boundary condition is solved by Fourier Galerkin methods given by $\frac{\partial}{\partial t}u_N = \epsilon^2\Delta u_N$. Then,*

$$\left|\left|\left|u_N(t,\cdot)\right|\right|\right|_p \le \left|\left|\left|u_N(0,\cdot)\right|\right|\right|_p$$

for any even positive integer p. Consequently, if the initial data $u_0 = u_0(x)$ satisfies $\left|\left|\left|P_N u_0\right|\right|\right|_p \le 1$ for all even number p, then the solution $u_N = u_N(t,\cdot)$ has the following uniform bound

$$\|u_N(t,\cdot)\|_\infty \le 1, \quad \forall t \ge 0.$$

3.3. Fourier collocation methods and the uniform L^2-bound. We turn to the semi-discrete Fourier collocation method for the Allen–Cahn equation with periodic boundary condition on domain $[0, 2\pi]$. We choose the discrete points as the Fourier collocation points in $[0, 2\pi]$, i.e. $x_j = \frac{2\pi j}{N}, j = 0, 1, \cdots, N-1$. Same as in the finite difference scheme, we use $U_j(t)$ to denote the approximation of $u(t, x_j)$, $U = (U_0, U_1, \cdots, U_{N-1})^T$, and $(U)^{\cdot k} = (U_0^k, U_1^k, \cdots, U_{N-1}^k)^T$. Though in this case, we use D_h^C to denote the differentiation matrix associated with Fourier spectral-collocation methods for the second order derivative. For more details, we refer to [22]. Then we end up with the following nonlinear ODE system

$$\begin{cases} \frac{dU}{dt} = \epsilon^2 D_h^C U + U - (U)^{\cdot 3}, \\ U(0) = U^0 = (u_0(x_0), u_0(x_1), \cdots, u_0(x_{N-1}))^T, \end{cases} \tag{27}$$

Since D_h^C is negative semidefinite, we have a similar result as Theorem 3 for Fourier collocation methods.

Theorem 4. *For the Allen–Cahn equation, if the initial data $u_0 = u_0(x)$ satisfies*

$$\left|\left|\left|U^0\right|\right|\right|_2 \le 1.$$

then the numerical solution $U(t)$ given by the Fourier collocation method (27) satisfies the uniform L^2-bound in the sense that

$$\left|\left|\left|U(t)\right|\right|\right|_2 \le 1, \quad \forall t \ge 0. \tag{28}$$

In this case, we observe that we are unable to derive the uniform L^p-bound for $p > 2$ due to the inequality that, for any $U \in R^N$ and all even number $p > 2$,

$$\left(U^{\cdot(2p-1)}\right)^T D_h^C U \not\le 0. \tag{29}$$

This is in contrast with Fourier Galerkin methods, for which the complication comes from the nonlinear term.

4. Fully discrete schemes and the uniform L^p-bound

Next we intend to consider fully discrete schemes for the Allen–Cahn equation that preserve some uniform L^p-bound. Based on the study of semi-discrete schemes in the previous section, we expect that the full discretization with finite difference spatial discretization may be able to preserve the numerical maximum principle, but not the Fourier Galerkin/collocation methods.

TABLE 1. Performances of four schemes over preserving numerical maximum principle.

Scheme	Linear/Nonlinear	Accuracy	Time step constraint
semi-implicit (30)	Linear	First-order	$\tau \leq \frac{1}{2}$
stabilized semi-implicit (31)	Linear	First-order	$\frac{1}{\tau} + \beta \geq 2$
convex splitting (32)	Nonlinear	First-order	Unconditionally
Crank-Nicolson (33)	Nonlinear	Second-order	$\tau \leq \min\{\frac{1}{2}, \frac{h^2}{2\epsilon^2}\}$

4.1. Time stepping schemes with discrete maximum principle. In this part, we consider the time discretization for the semi-discrete system (15). Several standard time-stepping schemes are able to preserve the uniform L^p-bound, including semi-implicit scheme

$$\frac{U^{n+1} - U^n}{\tau} = \epsilon^2 D_h U^{n+1} + U^n - (U^n)^{\cdot 3}, \tag{30}$$

stabilized semi-implicit scheme

$$\frac{U^{n+1} - U^n}{\tau} = \epsilon^2 D_h U^{n+1} - b(U^{n+1} - U^n) + U^n - (U^n)^{\cdot 3}, \quad b > 0 \tag{31}$$

convex splitting scheme

$$\frac{U^{n+1} - U^n}{\tau} = \epsilon^2 D_h U^{n+1} + U^n - (U^{n+1})^{\cdot 3}, \tag{32}$$

and second order Crank-Nicolson scheme

$$\frac{U^{n+1} - U^n}{\tau} = \epsilon^2 D_h \frac{U^{n+1} + U^n}{2} + \frac{U^{n+1} + U^n}{2} - \frac{(U^{n+1})^{\cdot 3} + (U^n)^{\cdot 3}}{2}. \tag{33}$$

The first two schemes are proved to preserve the numerical maximum principle under some time step constraint in [27]. The convex scheme can preserve the maximum principle unconditionally, which can be proved by following the techniques offered in [27]. The last scheme is also shown to preserve numerical maximum principle conditionally [18]. The table below is the summary of the properties and conditions associated to the above schemes.

4.2. The splitting method and uniform L^2-bound. For the spectral methods, we only take Fourier collocation methods as an example. We use operator splitting technique time discretization to solve the semi-discrete system (27). The ODE system can be split into two sub-problems involving the nonlinear part

$$A: \quad \frac{dV}{dt} = V - (V)^{\cdot 3}, \tag{34}$$

and the linear part

$$B: \quad \frac{dW}{dt} = \epsilon^2 D_h^C W. \tag{35}$$

To keep the presentation short, we denote $\mathcal{S}_t^A V_0$ to represent the solution of the Problem A at time t starting from initial value V_0 at time 0. Similarly, $\mathcal{S}_t^B W_0$ represents the solution of the Problem B at time t starting from initial value W_0 at time 0. Taking the similar notation in [3], we can obtain high order splitting methods in form

$$U^{n+1} = P_s U^n = \prod_{j=1}^{s} \mathcal{S}^B_{b_j\tau} \mathcal{S}^A_{a_j\tau} U^n = \mathcal{S}^B_{b_1\tau} \mathcal{S}^A_{a_1\tau} \mathcal{S}^B_{b_2\tau} \mathcal{S}^A_{a_2\tau} \cdots \mathcal{S}^B_{b_s\tau} \mathcal{S}^A_{a_s\tau} U^n, \tag{36}$$

where τ is the time step size. For example, when $s = 2$, $a_1 = a_2 = 0.5$, $b_1 = 1$ and $b_2 = 0$, this is the famous second order Strang splitting given in [25] as

$$U^{n+1} = P_2 U^n = \mathcal{S}^A_{\frac{\tau}{2}} \mathcal{S}^B_\tau \mathcal{S}^A_{\frac{\tau}{2}} U^n. \tag{37}$$

An example of fourth order splitting scheme can be found in [3, 26].

We note that the exact solutions of such splitting schemes are readily available since each of two sub-problems can be solved exactly with solutions given respectively by:

$$v_j^{n+1} = \mathcal{S}^A_\tau v_j^n = \frac{v_j^n}{\sqrt{e^{-2\tau} + (1 - e^{-2\tau})(v_j^n)^2}}, \quad j = 0, 1, \cdots, N-1, \tag{38}$$

to Problem A and

$$W^{n+1} = \mathcal{S}^B_\tau W^n = e^{\tau \epsilon^2 D_h^C} W^n, \tag{39}$$

to Problem B. The computation in (38) is point-wise computing with a cost of $\mathcal{O}(N)$ operations. One may apply FFT to handle the computation in (39) with a cost of $\mathcal{O}(N \log N)$ operations. These types of algorithms have been widely used before, see e.g., [2].

For the discrete form of average L^2-norm defined consistently with (4) as

$$|||u|||_2 = \frac{1}{2\pi} \|u\|_2^2 = \frac{1}{2\pi} \sum_{j=0}^{N-1} \frac{2\pi}{N} |u_j|^2 = \frac{1}{N} \sum_{j=0}^{N-1} |u_j|^2, \tag{40}$$

we assume that the initial data $U^0 = (u_0(x_0), u_0(x_1), \cdots, u_0(x_{N-1}))^T$ satisfy

$$|||u_0|||_2 = \frac{1}{N} \sum_{j=0}^{N-1} |u_0(x_j)|^2 \le 1. \tag{41}$$

By noticing that the function

$$g(\alpha) = \frac{\alpha}{e^{-2\tau} + (1 - e^{-2\tau})\alpha},$$

is monotone increasing and concave in $[0, +\infty)$, we have

$$\left|||V^{n+1}|||_2 = \frac{1}{N} \sum_{j=0}^{N-1} g((V_j^n)^2) \le g(|||V^n|||_2)\right. . \tag{42}$$

for the Problem A. Since $g(1) = 1$, it is easy to see from (42) that if V^n satisfies $|||V^n|||_2 \le 1$, then $\left|||V^{n+1}|||_2 \le 1\right.$. Meanwhile, it is quite obvious that

$$\left|||W^{n+1}|||_2 \le |||W^n|||_2, \tag{43}$$

since D_h^C is negative semidefinite. Combining (42) with (43) implies following theorem.

Theorem 5. *For the Allen–Cahn equation, if the initial data satisfy the assumption (41), then solution obtained by the fully discrete Strang splitting method defined as (37) satisfies the uniform L^2-bound in the sense that*

$$|||U^n|||_2 = \left|||(P_2)^n U^0|||_2 = \left|\left|\left|(\mathcal{S}^A_{\frac{\tau}{2}} \mathcal{S}^B_\tau \mathcal{S}^A_{\frac{\tau}{2}})^n U^0\right|\right|\right|_2 \le 1 \tag{44}$$

for all $n > 0$ with positive time step τ.

TABLE 2. Errors and convergence rates at $T = 1$ compared with reference solutions.

Order		$\tau = 0.2$	$\tau = 0.1$	$\tau = 0.05$	$\tau = 0.025$
2nd	Error	5.88e-7	1.47e-7	3.69e-8	9.23e-9
	Rate	-	1.995	1.999	2.000
4th	Error	6.68e-11	4.19e-12	2.54e-13	1.69e-14
	Rate	-	3.997	4.040	3.910
RK4	Error	9.92e-7	6.72e-8	4.37e-9	2.79e-10
	Rate	-	3.884	3.942	3.971

TABLE 3. Errors and convergence rates at $T = 10$ compared with reference solutions.

Order		$\tau = 0.2$	$\tau = 0.1$	$\tau = 0.05$	$\tau = 0.025$
2nd	Error	6.27e-3	1.59e-3	3.98e-4	9.95e-5
	Rate	-	1.984	1.996	1.999
4th	Error	5.48e-7	2.77e-8	1.61e-9	9.90e-11
	Rate	-	4.308	4.104	4.024

Remark 1. *If we use finite difference for the space discretization and Strang splitting method in time, we get two sub-problems*

$$A: \ \frac{dV}{dt} = V - (V)^{\cdot 3}, \qquad B: \ \frac{dW}{dt} = \epsilon^2 D_h W.$$

Clearly, if the initial value is bounded by 1*, the solution of problem A is entirely bounded by* 1*. From Lemma 2, the maximum value of the solution to problem B is no larger than the maximum value of initial value. This means if we solve the Allen–Cahn equation by this technique, we will achieve the discrete maximum principle unconditionally. Meanwhile, it is both second-order accurate in time and in space.*

5. Numerical tests

In this section, we carry out numerical experiments to verify our numerical analysis. Since standard time stepping scheme with spatial finite difference approximations have been studied in [27] and [18], we focus on the Fourier collocations for space and splitting scheme in time scheme. The scheme can be implemented efficiently as discussed previously.

5.1. Numerical results. Our analysis is independent of spatial dimensions, but for simplicity, we only consider a one-dimensional version of (1) with periodic boundary condition. The initial condition is chosen as

$$u_0(x) = 0.05 \sin(x).$$

The parameter ϵ^2 is 0.01, the computation domain is $[0, 2\pi]$ and the mesh size in space is $h = \frac{\pi}{64}$. We take solutions obtained by the fourth order Runge-Kutta (RK4) method with very small time step $\tau = 0.001$ as reference solutions to test convergence rates. The numerical results are showed in Table 2 and Table 3.

From the two tables, we can see that all numerical schemes achieve the optimal convergence rate. By comparing the two splitting schemes with each other, we see that the fourth order splitting scheme is much more accurate than the second order scheme. Furthermore, we can observe that among the two fourth order schemes, the splitting scheme can enhance the accuracy significantly over the standard RK4.

This can be attributed to the absence of other discretization errors at each time level except for the splitting error.

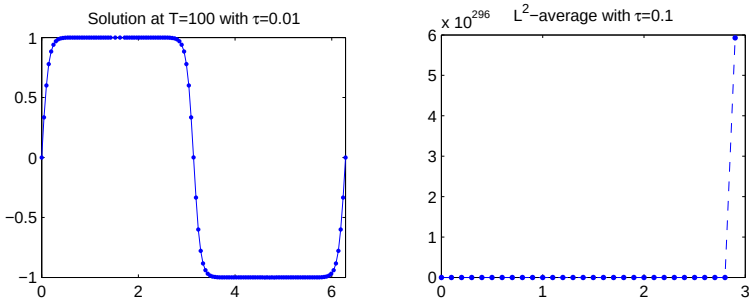

FIGURE 1. Solutions with fourth order Runge-Kutta methods.

We now study the performances of two splitting schemes in long time simulations with large time steps. We will use the L^2-average defined by (40) to measure the robustness of schemes. We also use the same example as above. First, we get a reference solution at $T = 100$ by RK4 with a small time step $\tau = 0.01$. Then for larger time steps, say $\tau = 0.1$, the L^2 norm blows up at $T = 3$ for RK4, which is presented in Fig. 1. On the other hand, we can find the splitting schemes allow much larger time steps.

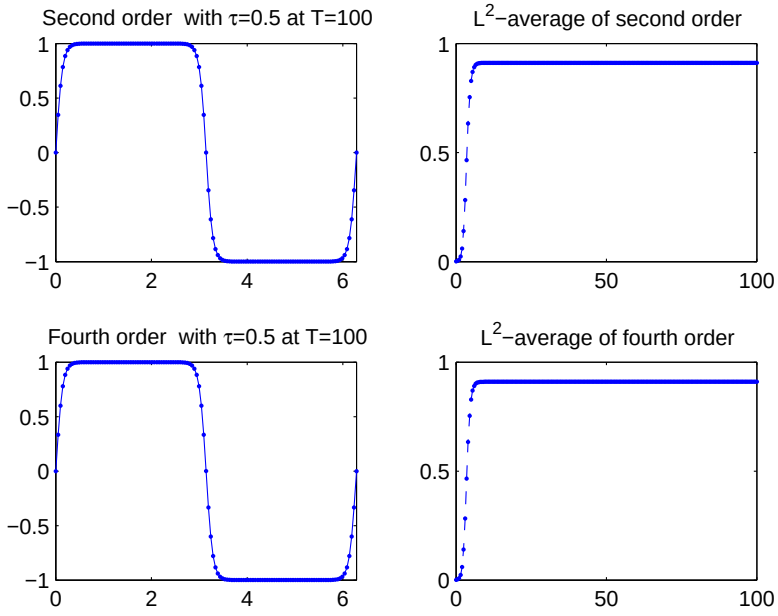

FIGURE 2. Solutions at $T = 100$ with $\tau = 0.5$ by two splitting schemes.

In Fig. 2, we observe that both splitting schemes work quite well for $\tau = 0.5$ in reaching a steady state solution and the L^2-average is uniformly bounded by 1. But when we enlarge the time step to $\tau = 2$ (shown in Fig. 3), the second order splitting scheme gives us nearly the same steady state as the one using a smaller step size but the fourth order splitting scheme gets totally wrong solutions. This

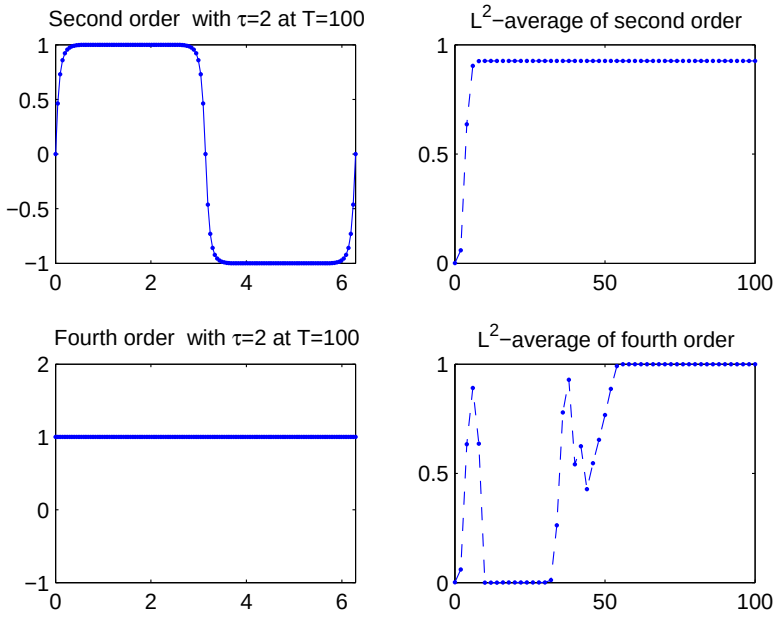

FIGURE 3. Solutions at $T = 100$ with $\tau = 2$ by two splitting schemes.

indicates that we might need some time step constraint to get the true steady state for fourth order splitting methods due to the appearance of negative fractional time steps. In experiments not reported here, we observe that the second order splitting scheme can guarantee the L^2-bound even when $\tau = 100$, which is in good agreement with the results of Theorem 5, but the fourth order schemes blows up very fast, indicating again that the latter, while more stable than RK4, are less stable than the second order counterpart.

6. Concluding remarks

In this work, a new uniform L^p-bound for the Allen–Cahn equation and its discretization schemes are presented, which differs from the conventional energy bound and maximum principle. Concerning practical fully discrete numerical schemes for the Allen–Cahn equation, due to the smoothness of phase field functions in space, it is well-known that high order time discretization tends to reduce the overall computational cost. In more recent years, high order in time disccretizations are also receiving more and more attention [19, 29]. Theoretical results presented in this work inform us that the second order Strang splitting scheme unconditionally preserves the uniform L^2-bound, hence it enjoys some forms of stability and has low computational cost. Extensive experiments also provide demonstrations of the effectiveness in combining high order time splitting schemes with Fourier collocation spatial discretization. This further motivates development of other high order schemes for Allen–Cahn and other interesting nonlinear dynamic systems in the future.

We end this paper with some discussions on the extension to vector-valued Allen–Cahn (Ginzburg-Landau) equations [6, 21], in which $\mathbf{u} : R^d \to R^d$ satisfies

$$\frac{\partial \mathbf{u}}{\partial t} = \epsilon^2 \Delta \mathbf{u} + \mathbf{u} - |\mathbf{u}|^2 \mathbf{u}.$$

Here $|\cdot|$ denotes the standard Euclidean norm in R^d. We can easily extend all theoretical results for the scalar-valued Allen–Cahn equations to vector-valued Ginzburg-Landau equations on both continuum level and discrete level since

$$(|\mathbf{u}|^2 u_k, u_k^{2p-1}) \geq (u_k^3, u_k^{2p-1})$$

always holds for each real-valued component u_k. Even for the operator splitting methods, the subproblem $\frac{\partial \mathbf{u}}{\partial t} = \mathbf{u} - |\mathbf{u}|^2\mathbf{u}$ can be solved in the explicit form

$$\mathbf{u}(t) = \frac{\mathbf{u}(0)}{\sqrt{e^{-2t} + (1 - e^{-2t})|\mathbf{u}(0)|^2}}.$$

It will be interesting to study similar investigations on other extensions of the Ginzburg-Landau and Allen–Cahn dynamics in the future.

Acknowledgments

The research was partially supported by the NSFC-91630207, U.S. NSF grants DMS-1558744, the AFOSR MURI center for Material Failure Prediction through Peridynamics and the ARO MURI Grant W911NF-15-1-0562.

References

[1] S.M. Allen and J.W. Cahn, A microscopic theory for antiphase boundary motion and its application to antiphase domain coarsening, Acta Metall, 27 (1979), 1085-1095.
[2] W. Bao, and Q. Du, Computing the ground state of the Bose-Einstein condensate via normalized gradient flow, SIAM J. Scientific Comp., 25 (2004), 1674-1697.
[3] S. Blanes, and P.C. Moan, Practical symplectic partitioned Runge-Kutta and Runge-Kutta-Nyström methods, J. Comput. Appl. Math., 142(2) (2002), 313-330.
[4] L. Chen, Phase-field models for microstructure evolution, Ann. Rev. Mater. Res., 32 (2002), 113-140.
[5] Q. Du, Discrete gauge invariant approximations of a time-dependent Ginzburg-Landau model of superconductivity, Math. Comp., 67 (1998), 965-986.
[6] Q. Du, Numerical approximations of the Ginzburg-Landau models for superconductivity, J. Math. Phys., 46 (2005), 095-109.
[7] Q. Du, M. Gunzburger, and J. Peterson, Analysis and approximation of the Ginzburg–Landau model of superconductivity, SIAM Rev., 34 (1992), 54-81.
[8] Q. Du and W. Zhu, Stability analysis and applications of the exponential time differencing schemes, J. Computational Mathematics, 22 (2004), 200-209.
[9] http://en.wikipedia.org/wiki/Circulant_ matrix.
[10] L.C. Evans, H.M. Soner, and P.E. Souganidis, Phase transitions and generalized motion by mean curvature, Commun. Pure Appl. Math., 45 (1992), 1097-1123.
[11] D.J. Eyre, An unconditionally stable one-step scheme for gradient systems, June 1998, unpublished, http://www.math.utah.edu/eyre/research/methods/stable.ps.
[12] X.B. Feng and A. Prohl, Numerical analysis of the Allen–Cahn equation and approximation for mean curvature flows, Numer. Math., 94(1) (2003), 33-65.
[13] X. Feng, H. Song, T. Tang and J. Yang, Nonlinearly stable implicit-explicit methods for the Allen–Cahn equation, Inve. Prob. Image, 7(3) (2013), 679-695.
[14] X. Feng, T. Tang and J. Yang, Stabilized Crank-Nicolson/Adams-Bashforth schemes for phase field models, East Asian J. Appl. Math., 3 (2013), 59-80.
[15] X. Feng, T. Tang and J. Yang, Long time numerical simulations for phase-field problems using p-adaptive spectral deferred correction methods, SIAM J. Sci. Comput., 37 (2015), A271-A294.
[16] L. Golubovic, A. Levandovsky and D. Moldovan, Interface dynamics and far-from-equilibrium phase transitions in multilayer epitaxial growth and erosion on crystal surfaces: Continuum theory insights, East Asian J. Appl. Math., 1 (2011), 297-371.
[17] J.S. Hesthaven, S. Gottlieb, and D. Gottlieb, Spectral methods for time-dependent problems, Vol. 21, Cambridge University Press, 2007.
[18] T. Hou, T. Tang and J. Yang, Numerical analysis of fully discretized Crank–Nicolson scheme for fractional-in-space Allen–Cahn equations, to appear in J Sci Comput (2017). doi:10.1007/s10915-017-0396-9.

[19] L. Ju, J. Zhang, L. Zhu and Q. Du, Fast explicit integration factor methods for semilinear parabolic equations, Journal of Scientific Computing, 62 (2015): 431-455.
[20] J. Kim, Phase-field models for multi-component fluid flows. Commun. Comput. Phys., 12 (2012), 613-661.
[21] J. Neu, Vortices in complex scalar fields, Physica D, 43 (1990), 385406.
[22] J. Shen, T. Tang, Spectral and high-order methods with applications. Science Press, 2006.
[23] J. Shen, T. Tang and J. Yang, On the maximum principle preserving schemes for the generalized Allen–Cahn equation, Comm. in Math. Sci., 14(6) (2016), 1517-1534.
[24] J. Shen and X. Yang, Numerical approximations of Allen–Cahn and Cahn-Hilliard equations, Discret. Contin. Dyn. Syst. , 28 (2010), 1669-1691.
[25] G. Strang, On the construction and comparison of difference schemes, SIAM J. Numer. Anal., 5.3 (1968), 506-517.
[26] M. Suzuki, General theory of fractal path integrals with applications to many-body theories and statistical physics, J. Math. Phys., 32 (1991): 400.
[27] T. Tang and J. Yang, Implicit-explicit scheme for the Allen–Cahn equation preserves the maximum principle, J. Comput. Math., 34(5) (2016), 471-481.
[28] X. Yang, Error analysis of stabilized semi-implicit method of Allen–Cahn equation, Discrete Contin. Dyn. Syst. Ser. B, 11(4) (2009), 1057-1070.
[29] J. Zhang and Q. Du, Numerical studies of discrete approximations to the Allen–Cahn equation in the sharp interface limit, SIAM J. Sci. Comput., 31(4) (2009), 3042-3063.

Department of Mathematics, Southern University of Science and Technology, Shenzhen, Guangdong, China
E-mail: yangj7@sustc.edu.cn

Department of Applied Physics and Applied Mathematics, Columbia University, New York, US,
E-mail: qd2125@columbia.edu

Beijing Computational Science Research Centre, Beijing, P.R. China, & Division of Science and Technology, Beijing Normal University - Hong Kong Baptist University United International College, Zhuhai, Guangdong, China
E-mail: wzhang@csrc.ac.cn